Published in final edited form as:
Phys Rev Lett. 2006 March 3; 96(8): 088306.

Excluded-Volume Effects in Tethered-Particle Experiments: Bead Size Matters

Darren E. Segall[1], **Philip C. Nelson**[2], and **Rob Phillips**[3]

[1]Division of Engineering and Applied Science, California Institute of Technology, Pasadena, CA 91125 USA

[2]Department of Physics and Astronomy, University of Pennsylvania, Philadelphia PA 19104, USA

[3]Division of Engineering and Applied Science and Kavli Nanoscience Institute, California Institute of Technology, Pasadena, CA 91125 USA

Abstract

The tethered-particle method is a single-molecule technique that has been used to explore the dynamics of a variety of macromolecules of biological interest. We give a theoretical analysis of the particle motions in such experiments. Our analysis reveals that the proximity of the tethered bead to a nearby surface (the microscope slide) gives rise to a volume-exclusion effect, resulting in an entropic force on the molecule. This force stretches the molecule, changing its statistical properties. In particular, the proximity of bead and surface brings about intriguing scaling relations between key observables (statistical moments of the bead) and parameters such as the bead size and contour length of the molecule. We present both approximate analytic solutions and numerical results for these effects in both flexible and semiflexible tethers. Finally, our results give a precise, experimentally-testable prediction for the probability distribution of the distance between the polymer attachment point and the center of the mobile bead.

Single-molecule biophysics has rapidly become an experimental centerpiece in the dissection of cellular machinery. This part of the biophysics repertoire often relies, in turn, on the use of micron-scale beads both as a reporter of underlying molecular motions and as the “handle” for grabbing these single-molecule systems. Thus, a key part of the theoretical infrastructure of this field is a clear understanding of the role that these beads play in altering the statistical properties of the macromolecules which are the real target of interest in such experiments.

Beyond interest in the *in-vitro* consequences of tethered-particle motions, many processes within the cell themselves involve tethering. A notable example has to do with vesicular trafficking, in which molecular motors [1] carry tethered cargoes with similar Earth-like proportions relative to the molecular Atlases doing the heavy lifting. Thus, the statistical-mechanical analysis performed here may prove useful for understanding *in-vivo* processes, in addition to the *in-vitro* consequences that form the main motivation for the work.

Figure 1 sketches the tethered particle method (TPM). The main idea is that a macromolecule (for example DNA or some protein that translocates DNA or RNA) is anchored at one end to a surface, while the other end of the molecular complex is attached to a bead. The observed motion of the bead serves as a reporter of the underlying macromolecular motion. This technique has been used in a variety of settings *e.g.* the examination of nanometer-scale motions of motors like kinesin [2] or RNA polymerase [3, 4], protein synthesis by ribosomes [5], exonuclease translocation on DNA [6, 7]; protein mediated deformation [8] and loop formation [9] in DNA, DNA hybridization [10] and DNA motion [11, 12]. The main goal of this paper is to show how the proximity of the

reporter bead to the surface affects the interpretation of the reported data and can even alter the conformation of the macromolecule of interest. A theoretical understanding of these effects will improve the ability to use the TPM for quantitative [13] analysis of biomolecular properties at the single molecule level.

In the remainder of the paper, we first describe a simple statistical-mechanical theory of bead-induced volume-exclusion forces. We show how these forces depend both upon bead size and on tether length. We also derive scaling relations between the experimental measurables (bead position) and parameters such as bead size and tether length. Because the simple analytic model neglects some features of the full problem, we then turn to simulation results which capture all of the key effects and compare to the analytic results.

The aim of the calculations outlined below is to illustrate how the presence of a bead alters the statistical properties of the molecule to which it is tethered and how the bead reports information to the experimenter. We confine our discussion to the equilibrium characteristics of this phenomenon, a key measurable in TPM experiments even for the study of dynamical processes [3–7, 9, 11]. We first note that in many experiments, the bead is flexibly linked to the end of its molecular tether, and hence is nearly free to rotate around the point of linkage [4, 12]. However, steric constraints limit this freedom. In particular, the closer the bead is to the surface, the fewer angular conformations are available to it (Fig. 1).

The statistical properties of the bead in TPM are determined by the coarse-grained free energy function (or “Hamiltonian”)

$$H=H_m(\{X\})+H_{b,m}(\mathbf{R},\{X\})+H_b(\mathbf{R},\{X\}). \quad (1)$$

Here $\{X\}$ is an abstract set of coordinates describing the configuration of the molecule and $\mathbf{R}$ is the vector pointing from the end-point of the molecule to the center of the bead (Fig. 1). Eq. 1 contains three terms: The first describes the self-interactions of the molecule and interactions with external forces (surface forces or applied fields) other than those with the bead itself. Those interactions are captured by the second term, $H_{b,m}$. The last term, H_b, describes the external forces on the bead, for example those arising from applied fields or the surface. This term also depends on the configuration of the molecule, as the position of the bead depends on both its orientation $\mathbf{R}$ and the molecule’s end-point.

We obtain the statistical average of an observable A of the system as a weighted average over all the configurations of the system

$$\langle A\rangle=\frac{1}{Z}\int d\{X\}d^2\widehat{\mathbf{R}}A(\{X\},\mathbf{R})\,e^{-\beta H}.$$

Here $\int d^2\hat{\mathbf{R}}$ is an integral over bead orientations and Z is the partition function.

Before discussing the consequences of this model, we first discuss the significance of the terms in Eq. 1 and make some initial simplifications. The external forces acting on the bead that we have in mind result from its interaction with the surface. This interaction contains the repulsive double layer potential and an attractive van der Waals interaction [14], along with a hard-wall repulsion (Eq. 2 below). Under physiological conditions, the double layer potential has an interaction range with a typical length scale of a nanometer, much shorter than the molecule lengths of interest to us; the van der Waals attraction, too, is weak on long scales [15]. Accordingly, we will model all bead–wall interactions using a simple hard-wall potential. We will also temporarily ignore bead–molecule interactions; later we will show

that they have little influence for tethers like the ones of interest here. Given these assumptions, the last two terms in Eq. 1 simplify to

$$H_{b,m}=0, \quad H_b=\begin{cases} 0 & \text{if } R(1-\cos(\alpha))<z \\ \infty & \text{if } R(1-\cos(\alpha)) \geq z, \end{cases} \tag{2}$$

where z is the height of the end-point of the molecule and α is the polar angle of **R** (Fig. 1).

We now examine the statistical averages of a molecular property $A_m(\{X\})$ such as end-to-end distance. To obtain the average value of $A_m(\{X\})$, not only do we need to sum over all of the configurations of the molecule, but also, we must sum over all of the configurations of the bead. Thanks to the simplifications in Eq. 2, the integration over **R** can be done explicitly and results in an *effective* free energy function for the molecule. That is, the resulting statistical average of A_m can be written as

$$\langle A_m \rangle = \frac{1}{Z} \int d\{X\} A_m(\{X\}) e^{-\beta H_{\text{eff}}}, \text{ where} \tag{3}$$

$$H_{\text{eff}} = H_m(\{X\}) - k_B T \log(\Omega(z)). \tag{4}$$

The new second term in H_{eff} accounts for the configurations available to the bead. $\Omega(z)$ is the solid angle allowed for **R**, given a molecular configuration $\{X\}$:

$$\Omega(z)=\begin{cases} 2\pi z/R, & z<2R \\ 4\pi, & z \geq 2R. \end{cases} \tag{5}$$

The partition function is also consistent with the definition of the effective Hamiltonian, $Z = \int d\{X\} e^{-\beta H_{\text{eff}}}$.

As a result of the constraints on the excursions of the bead there is an effective repulsive force, which prevents the end-point of the molecule from making contact with the surface and stretches the molecule. That is, the problem is equivalent to one without the bead, but in which the end-point of the molecule is subjected to a force

$$\mathbf{F}_{\text{eff}} = z^{-1} \Theta(2R - z) k_B T \, \hat{\mathbf{k}}, \tag{6}$$

where Θ is the Heaviside step function. This entropic force alters the statistical properties of the tethered molecule (Eq. 3), and can affect its interactions with itself or with other molecules.

The key measurable associated with current TPM experiments is the position of the bead itself. That is, the output of the experiment is a record of the positions of the bead on successive video frames [5, 11, 12, 16]. Having revealed that the confinement of the bead subjects the molecule to an entropic force, we now determine how this confinement influences bead motion. Note that one of our key conclusions is that there is a subtle dependence of the measured bead excursions on the size of the bead itself. To see this, let **r** (Fig. 1) denote the vector from the wall attachment point to the bead center. Given our simplifications (Eq. 2), the non-zero statistical moments of **r**, up to second order, are

$$\langle r_z\rangle=\langle z\rangle-\frac{1}{2}\langle z\rangle_\Theta+R\langle 1\rangle_\Theta \tag{7a}$$

$$\langle r_z^2\rangle=\langle z^2\rangle-\frac{2}{3}\langle z^2\rangle_\Theta+R\langle z\rangle_\Theta+R^2\left(\frac{1}{3}+\frac{2}{3}\langle 1\rangle_\Theta\right) \tag{7b}$$

$$\langle \mathbf{r}_\perp{}^2\rangle=\langle \mathbf{x}_\perp{}^2\rangle-\frac{1}{3}\langle z^2\rangle_\Theta+R\langle z\rangle_\Theta+\frac{2}{3}R^2\left(1-\langle 1\rangle_\Theta\right) \tag{7c}$$

where $\mathbf{r}_\perp$ is the in-plane displacement of the bead center and ($\mathbf{x}_\perp$; z) is the displacement of the end-point of the molecule. Here all quantities averaged on the right-hand side are independent of the coordinates of the bead and, hence, are defined as in Eq. 3. The averages with subscript Θ correspond to summing over states only when the end-point satisfies $z < 2R$, *i.e.*

$$\langle A_m\rangle_\Theta=\frac{1}{Z}\int d\{X\}A_m(\{X\})e^{-\beta H_{\text{eff}}}\Theta(2R-z). \tag{8}$$

These Θ-weighted terms arise because of the reduction of the configurations available to the bead due to the proximity of the surface (Eq. 5). Below it is shown how they give rise to experimentally testable scaling relations relating the excursion of the bead to its radius and the contour length of the molecule.

We further pursue an analytic description of TPM by modeling the molecule as a Gaussian chain. The Gaussian chain is a useful approximation for molecules with short persistence lengths (such as RNA) and we demonstrate, using numerical simulations, that it also serves as a good guide for semi-flexible molecules (*e.g.* DNA) in the regime of interest here.

Our problem involves a molecule grafted onto a surface, *i.e.* confined to a half space. DiMarzio showed that the corresponding Gaussian chain is described by [17]

$$H_{\text{m}}=(3k_{\text{B}}T/4L\xi)\left(\mathbf{x}_\perp{}^2+z^2\right)-k_{\text{B}}T\log(z/\ell). \tag{9}$$

L is the contour length of the molecule, ξ is the persistence length and ℓ is an arbitrary constant. The material properties of the molecule enter H_{m} only through the combination $L\xi$.

Because there are only two relevant length scales in the problem (R and $\sqrt{L\xi}$), we may write each moment of the molecule's excursions in terms of a function of a single variable. Using Eq. 9 to evaluate the averages in Eqs. 7:

$$\frac{\langle r_z\rangle}{\sqrt{L\xi/3}}=\frac{2(1-e^{-N_{\text{R}}^2})}{\sqrt{\pi}\,\text{erf}(N_{\text{R}})}+N_{\text{R}}\frac{2-\text{erf}(N_{\text{R}})}{\text{erf}(N_{\text{R}})}, \tag{10a}$$

$$\frac{\langle r_z^2\rangle}{L\xi/3}=2+\frac{4N_R}{\sqrt{\pi}\,\mathrm{erf}(N_R)}+N_R^2, \tag{10b}$$

$$\frac{\langle \mathbf{r}_\perp^2\rangle}{L\xi/3}=2+\frac{4N_R}{\sqrt{\pi}\,\mathrm{erf}(N_R)}. \tag{10c}$$

The excursions depend on the dimensionless number $N_R \equiv R/\sqrt{L\xi/3}$, which we call the "excursion number." N_R controls the bead's scaling behavior, defining regimes of molecule-dominated motion ($N_R < 1$) and bead-dominated motion ($N_R > 1$, confined rotations).

Figure 2 shows the relationship between excursions and N_R. For small excursion number, the excursions scale as $\langle r_z^2\rangle \approx \langle \mathbf{r}_\perp^2\rangle \approx L\xi$ and $\langle r_z\rangle \approx \sqrt{L\xi}$; the dependence on contour length obeys the expected relations for a Gaussian chain with no bead attached. The scaling changes for large excursion number. Now, the mean excursions display power-law dependences on N_R: $\langle \mathbf{r}_\perp^2\rangle \approx R\sqrt{L\xi}$, $\langle r_z^2\rangle \approx R^2$ and $\langle r_z\rangle \approx R$; the observed motion is dominated by the bead's rotation. The power law difference on bead radius R follows directly from the general relations (Eq. 7), independent of the model representing the molecule. Now, the in-plane excursions show a square-root dependence on the contour length, in contrast with the linear dependence for small excursion number. This functional form arises because the average height of the molecule (which depends on $\sqrt{L\xi}$) dictates the degree to which the bead can rotate. These scaling relations should be testable in experimental studies, where excursion numbers have ranged over wide set of values, $0.1 \le N_R \le 90$ [3–5, 8–11]. (Most are in the regime $N_R > 1$.)

Confinement effects can alter molecular properties, causing out-of-plane stretching of the molecule.

$$\frac{\langle z^2\rangle}{L\xi/3}=6-\frac{4}{\sqrt{\pi}}\frac{N_R e^{-N_R^2}}{\mathrm{erf}(N_R)}. \tag{11}$$

In contrast, a Gaussian chain in free solution has squared out-of-plane excursions of the molecule equal to $\langle z^2\rangle/(L\xi/3) = 2$. For many experiments [4–6, 8–11] the excursion number is such that the second term in Eq. 11 is negligible and the effects of bead exclusion (Eq. 6) and molecule exclusion (second term in Eq. 9) result in a tripling of the out-of-plane squared displacement of the molecule. (Both exclusion effects contribute equally.) The bead-induced stretching can be viewed as a consequence of the effective force (Eq. 6). In the Gaussian chain model, this force is

$$\langle F_{\mathrm{eff}}\rangle=\frac{k_B T}{\sqrt{\pi}\,\sqrt{L\xi/3}}\left(\frac{1-e^{-N_R^2}}{\mathrm{erf}(N_R)}\right). \tag{12}$$

This force can significantly affect rates of loop formation in DNA. Finzi and Gelles [9] used TPM to observe loop formation in DNA generated by the lac-repressor protein. Under their conditions, we predict an average effective force $\langle F_{\mathrm{eff}}\rangle \approx 25$ fN. Using the simple approximation that the rate of loop formation decreases by $\exp(-\beta\langle F_{\mathrm{eff}}\rangle l)$ (l is the operator-

operator distance) we estimate that the bead-confinement effect reduces the rate of loop formation by a factor of 2.

To check the validity of our simplified model, we performed a simple Monte Carlo calculation. Our results agree with an independent calculation by D. Brogioli [12]. Our code generated sets of discrete chains with random bends chosen to obtain a desired persistence length ξ. Each chain began at a random angle relative to the wall, and ended with the bead at a random orientation. Configurations where the bead, wall, or chain overlapped were discarded, (this includes bead-molecule interactions ($H_{b,m} \neq 0$)) and the required averages were computed. Figure 2 shows that even for a stiff polymer like DNA, the scaling relations predicted by the approximate analytical theory are accurate in the regime of interest to us. Actual experimental data allow the calculation of more subtle metrics than just averages, however: Fig. 3 shows predictions for the full probability distribution of excursions. The distribution is quite different from a Gaussian, a fact already observed experimentally [11].

The above results are interesting as fundamental polymer physics. For example, single-particle tracking allows the observation of the full probability distribution, and hence the opportunity to directly observe an end-end distribution for a semiflexible polymer and compare to our predictions. But our main goal was to develop a theoretical framework which can bolster the quantitative capabilities of the TPM—a relatively noninvasive, single molecule probe. We revealed that the proximity of the bead to the surface provokes an effective force on the molecule, altering its statistical properties and influencing biomolecular interactions. In addition, we determined how the excursions of the bead are influenced by experimental parameters such as bead size and contour lengths; relations which are currently being tested [16]. Finally, understanding how the competition between bead and tether effects is controlled by the excursion number N_R may help in the choice of optimal bead size and tether length for a given experiment.

Acknowledgments

We thank J. Beausang, S. Blumberg, D. Brogioli, D. Chow, D. Dunlap, L. Finzi, J. Gelles, Y. Goldman, I. Kulic, J.C. Meiners, T. Perkins, P. Purohit, F. Vanzi, P. Wiggins, C. Zurla, for extensive discussions. DS acknowledges the support of AFOSR/DARPA grant F49620-02-1-0085. RP acknowledges the support of the NIH Director's Pioneer Award DP1 OD000217 and NSF grant CMS–0301657. PN acknowledges the Human Frontier Science Foundation and NSF grant DMR–0404674.

References

1. Hirokawa N, Takemura R. Nat. Rev. Neurosci. 2005; 6:201. [PubMed: 15711600]
2. Gelles J, Schnapp BJ, Sheetz MP. Nature. 1988; 331:450. [PubMed: 3123999]
3. Schafer DA, Gelles J, Sheetz MP, Landick R. Nature. 1991; 352:444. [PubMed: 1861724]
4. Yin H, Landick R, Gelles J. Biophys. J. 1994; 67:2468. [PubMed: 7696485]
5. Vanzi F, Vladimirov S, Knudsen CR, Goldman YE, Cooperman BS. RNA. 2003; 9:1174. [PubMed: 13130131]
6. Dohoney KM, Gelles J. Nature. 2001; 409:370. [PubMed: 11201749]
7. van Oijen AM, Blainey PC, Crampton DJ, Richardson CC, Ellenberger T, Xie XS. Science. 2003; 301:1235. [PubMed: 12947199]
8. Dixit S, Singh-Zocchi M, Hanne J, Zocchi G. Phys. Rev. Lett. 2005; 94 118101.
9. Finzi L, Gelles J. Science. 1995; 267:378. [PubMed: 7824935]
10. Singh-Zocchi M, Dixit S, Ivanov V, Zocchi G. Proc. Natl. Acad. Sci. USA. 2003; 100:7605. [PubMed: 12808129]
11. Pouget N, Dennis C, Turlan C, Grigoriev M, Chandler M, Salomé L. Nucl. Acids Res. 2004; 32:e73. [PubMed: 15155821]
12. Brogioli D, Zurla C, Nelson PC, Dunlap DD, Finzi L. in preparation.

13. Earlier theoretical work 18 discussed an earlier version of the experimental technique, in which only the blurred image of the bead was observed. However, in that work bead-wall exclusion effects were neglected, critical for the analysis of tethered-particle experiments. In addition, recent experiments combine a tethered particle with single-particle tracking [5, 11, 12, 16], requiring analysis such as that presented here
14. Israelachvili, J. Intermolecular and Surface Forces. London: Academic Press; 1991.
15. Dagastine RR, Bevan M, White LR, Preive DC. J. Adhesion. 2004; 80:365.
16. Gelles J, Meiners JC, Finzi L, Phillips R. (private communications).
17. DiMarzio EA. J. Chem. Phys. 1965; 42:2101.
18. Qian H, Elson EL. Biophys. J. 1999; 76:1598. [PubMed: 10049340]

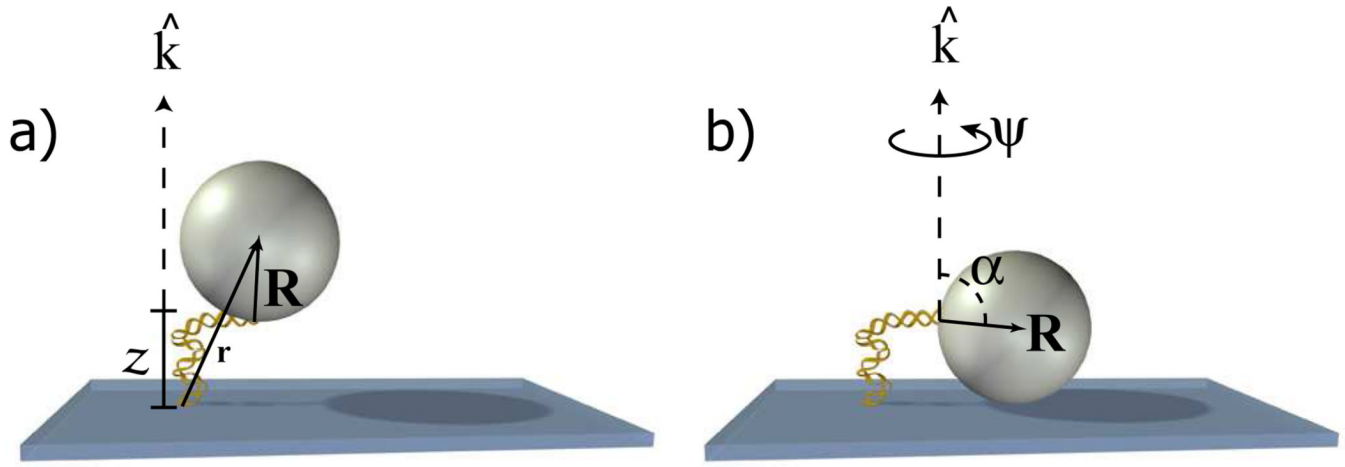

FIG. 1.

Schematic showing the tethered particle method. (a) The tether is attached to a specific point on the bead; *z* is the height of this point. **r** denotes the position of the center of the bead. (b) The vector **R** from the attachment point to the bead center can rotate and is described by two angles. These rotations are more constrained for small values of *z*. Note that in the figure the width of DNA is not to scale, it is much smaller in real experiments.

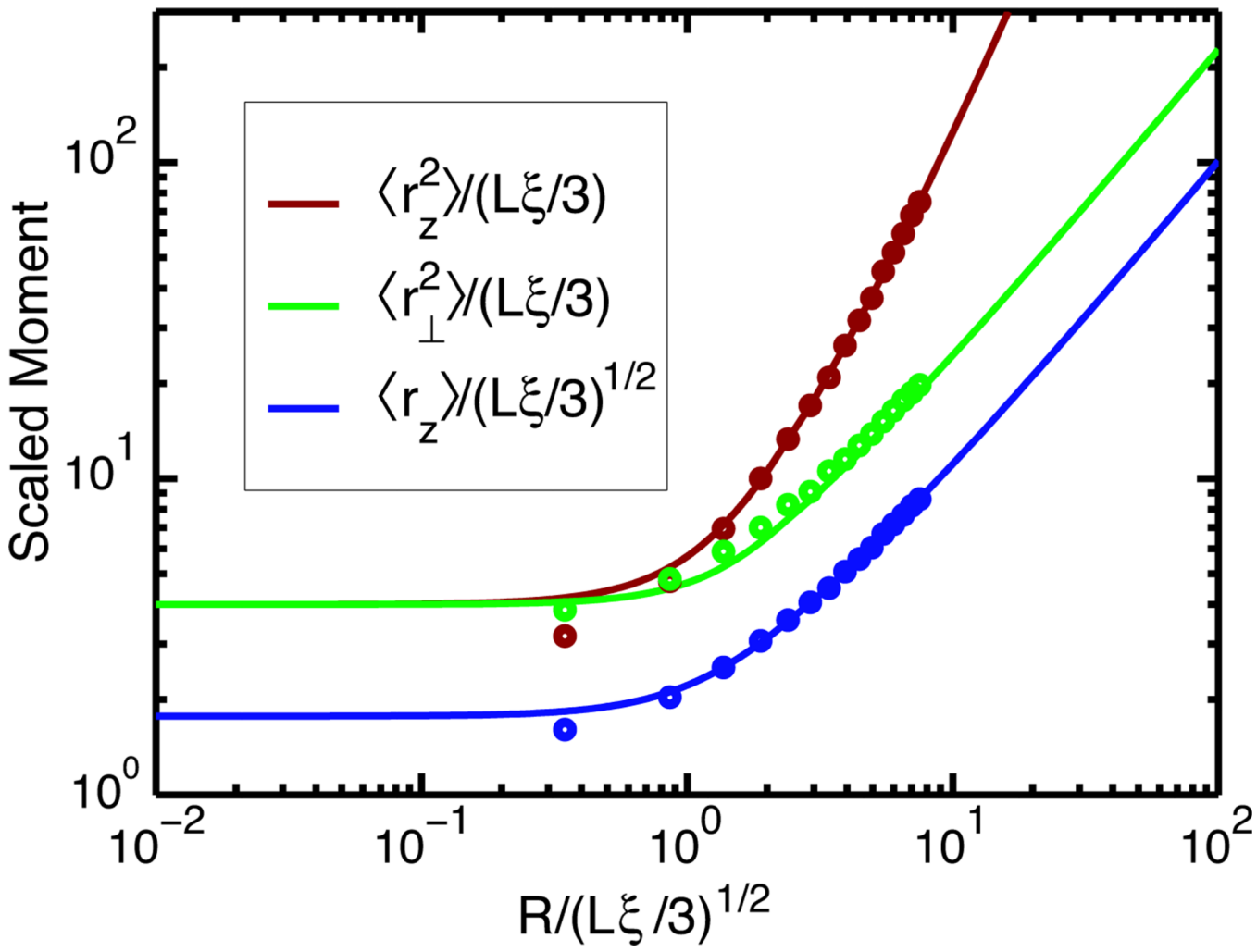

FIG. 2.

Scaling behavior of bead excursion, normalized by coil size parameter, versus the excursion number N_R. *Curves:* analytical theory in the Gaussian-chain approximation (Eq. 10). *Circles:* Monte Carlo calculation for a semiflexible chain with ξ = 50 nm, L = 1245 bp, and various values of R.

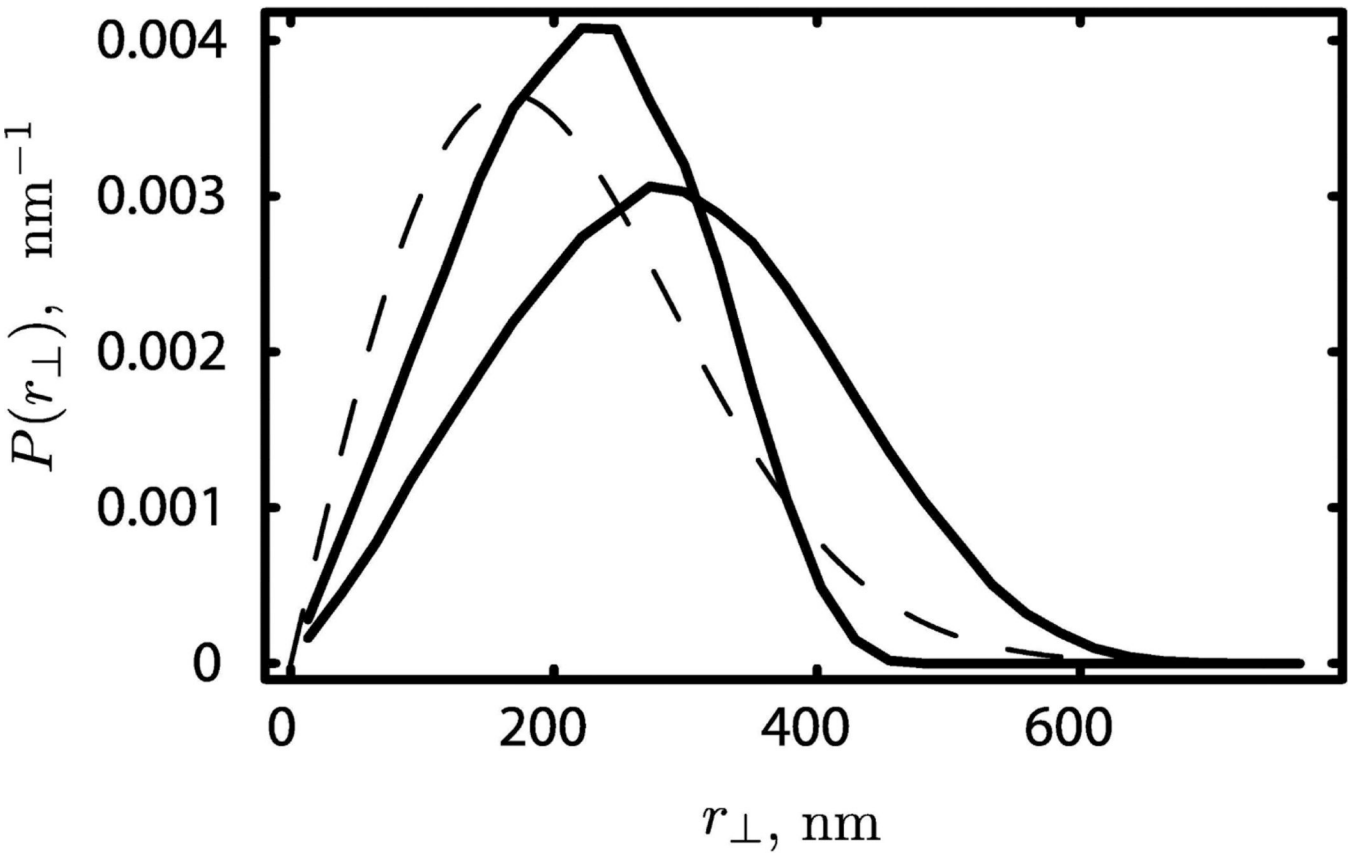

FIG. 3.

Solid curves: Theoretical prediction of the probability distributions for the projected distance **r**⊥, taking bead radius R = 250 nm, persistence length ξ = 50 nm, and contour length L = 1000 bp (left curve) and 2000 (right curve). *Dashed curve:* Two dimensional Gaussian distribution with the same mean-square excursion as the left curve.